



<https://doi.org/10.31217/p.40.1.3>

Failure Behavior Analysis of Crack Propagation in Ship Sandwich Structures

Husein Syahab^{1,2}, Achmad Zubaydi^{1*}, Heni Siswanti^{3,4}, Rizky Chandra Ariesta¹

¹ Department of Naval Architecture, Institut Teknologi Sepuluh Nopember, Surabaya, Indonesia

² Department of Naval Architecture, Institut Teknologi Kalimantan, Balikpapan, Indonesia

³ Department of Marine Technology, Politeknik Negeri Madura, Sampang, Indonesia

⁴ Department of Ocean Engineering, Institut Teknologi Sepuluh Nopember, Surabaya, Indonesia

* e-mail: zubaydi@its.ac.id (Corresponding author)

ARTICLE INFO

Original scientific paper

Received 21 May 2025

Accepted 6 July 2025

Key words:

Crack propagation

Finite element method

Sandwich plate

Ship structure

Strength reduction factor

ABSTRACT

Damage to ship structures leads to a reduction in strength, which increases the risk of structural failure. The vulnerability of damage in sandwich panel structures made of low-density steel-polyurethane elastomer needs to be evaluated and predictions made regarding failure modes, particularly crack propagation through the core thickness. Variations in structure thickness and the size of the initial crack are evaluated to determine the impact of structural design on damage under the ship's operational loads. Finite element analysis, validated with experimental data, is used to simulate the dynamics of crack propagation. It was found that a thicker core and a smaller initial crack length result in slower crack propagation rates and shorter crack extensions. Increasing the core thickness from 15 mm to 24 mm reduced the crack propagation rate by up to 28% and improved crack extension resistance by as much as 54%. Thicker face and bottom plates further contributed an additional reduction in crack growth rate, providing an extra margin of structural toughness. Shorter initial cracks also proved significant, with propagation rates decreasing by about 73% when comparing a 25 mm crack to a 75 mm crack. These factors lowered the strength reduction factor (SRF) and extended crack growth times, confirming that thicker cores and smaller initial cracks improve damage resistance in ship sandwich structures.

1 Introduction

The adoption of sandwich materials has proven to be a better alternative to conventional steel in ship structure. Notably, polyurethane elastomeric material has emerged as an efficient core material in such structures [1]. However, as their use grows, so does the need for understanding damage behavior, especially under static and dynamic ship loads. Common issues in sandwich materials include delamination and facesheet-core debonding, both of which compromise structural strength. Crack initiation often caused by stress exceeding design limits can accelerate failure [2]. Investigating damage tolerance is vital for determining service life and ensuring structural integrity, especially as core cracks pose significant risks and may originate near

joints subjected to fluctuating wave loads and water pressure [3, 4].

A fracture analysis approach, as outlined by Zenkert et al. [5], begins with examining material fracture properties and extends to plate-level and full-structure behavior. Ariesta et al. [6] used Experimental Modal Analysis (EMA) on side plates to evaluate dynamic responses to vibration-induced damage. Ismail et al. [7] expanded this by analyzing the effects of damage size and location in sandwich plates. At full scale, damage propagation can compromise the vessel's overall strength. Ismail et al. [8] found damage-induced frequency deviations in ro-ro ship ramps, while Ariesta et al. [9] showed how damage alters mode shapes in sandwich plates. Odessa et al. [10] investigated interfacial crack propagation, highlighting structural deformation

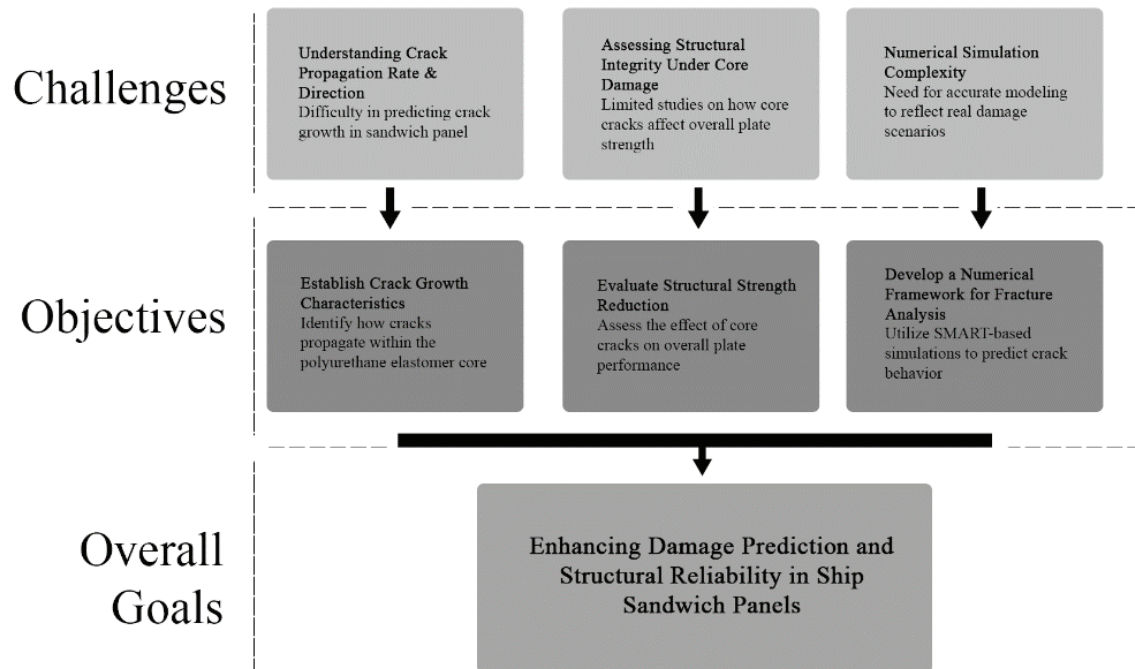


Figure 1 Challenges and Objectives in the research field

risks. Wang et al. [11] experimentally validated failure behavior, linking visual damage to strength reduction, further backed by numerical simulations.

Despite extensive research, gaps remain. Ismail et al. [1] assessed fiberglass-reinforced polyurethane elastomer's mechanical properties, but ignored fatigue or marine durability. Li et al. [12] studied impact resistance of polyurethane-steel composites but lacked long-term durability analysis. Chernysh and Yakovlev [13] linked deformation to contact conditions but did not consider environmental effects. In ship structures, Ismail et al. [14] demonstrated improved strength in SPS hulls but omitted fatigue analysis. Sharma et al. [15] and Khan et al. [16] analyzed fatigue life in various composites but without real-structure validation or fracture mechanism focus. Recent work by Ariesta et al. [17] and Dhaliwal et al. [18] addressed failure configurations and damage modes but lacked simulations and comprehensive crack placement analysis. Shen et al. [19] discussed core failures like delamination and debonding without numerical modeling. Kashani et al. [20] used XFEM for crack analysis, yet didn't connect findings to ship applications. SMART-based studies by Thiruvannamalai et al. [21] and Savari [22] analyzed fatigue life and crack behavior in FRP systems but missed strength degradation insights.

This study investigates the crack propagation behavior in polyurethane-steel sandwich panels, focusing on the impact of core thickness, initial crack length, and loading conditions on structural integrity. The framework presented in Figure 1 illustrates the key aspects of this research, categorizing the challenges, objectives, and

the overall goal. The challenges highlight existing gaps in understanding crack growth mechanisms, structural integrity assessment, and the complexity of numerical modeling. To address these, the objectives aim to characterize crack growth, evaluate strength reduction, and develop a reliable numerical framework. These objectives collectively contribute to the overall goal of enhancing damage prediction and structural reliability in ship sandwich panels. The flowchart below provides a structured representation of these elements, establishing a systematic approach for analysis and solution development. Therefore, the fracture analysis is carried out to identify the characteristics of sandwich panels in ship side structures when crack propagation occurs. The study involves plate panel modelling to its actual size and simulating the damage event for numerical analysis. The objectives of this research are to determine the rate and direction of crack propagation in sandwich panels used in ships and to assess the impact of crack damage on the strength of sandwich panels employed in ship construction. The study is conducted using numerical simulations focuses on sandwich plate panels used in ship side structures, and the crack propagation damage is assumed to be singular, occurring in the core with an initial crack provided.

2 Object Study and Methods

2.1 Research Methodology

The methodology employed in this study is structured to analyze the crack propagation behavior and its

effects on structural integrity in ship sandwich plate constructions. To prepare the analysis, a 3D structural model of the sandwich panel is created, consisting of steel faceplates and a polyurethane elastomer core. Finite element analysis (FEA) is then applied, where mesh generation, boundary conditions, and initial crack configurations are defined. To ensure the reliability of the simulation, a convergence study is conducted to validate mesh sensitivity and simulation stability; only upon achieving a convergent model does the study proceed to the crack propagation simulation stage.

Crack propagation is analyzed using the SMART fracture method, which enables adaptive remeshing around the crack tip to accurately simulate growth under quasi-static loading conditions [23]. SMART (Separating Morphing and Adaptive Remeshing Technology) is utilized in this study due to its proven effectiveness in simulating crack propagation, particularly in complex structures where crack paths are not predetermined. The method allows the observation of how cracks initiate and evolve under operational loading by inserting various initial crack lengths within the sandwich panel's core. This enables the identification of propagation trends, including direction and rate, which are essential for evaluating how different design configurations respond to damage. To assess the structural implications of crack growth, the study applies a comparative evaluation of structural strength before and after damage, using a strength reduction metric. Rather than comparing this reduction to a fixed allowable threshold, the analysis emphasizes relative differences across design variations such as differing faceplate and core thicknesses or initial crack sizes. This comparative approach aligns with established practices in composite structure evaluation, allowing for practical insights into which configurations offer better durability and resistance to damage. As a result, the methodology supports early-stage design decisions by identifying structural layouts that minimize degradation and improve overall resilience.

However, several limitations are acknowledged. The numerical modeling focuses solely on the polyurethane core subjected to converted loads, without including the steel faceplates and stiffening components. This simplification may overlook crucial interactions in stress redistribution and load transfer paths, a limitation similarly identified by Lameiras et al., [24] in comprehensive sandwich panel analyses. Additionally, while the study quantifies propagation time and strength

reduction, it does not delve into the finer-scale degradation mechanisms at the crack tip, such as matrix micro-cracking or plastic zone evolution. Such phenomena have been shown to play significant roles in energy dissipation during fatigue, as demonstrated by Nozaki et al., [25]. Moreover, the analysis is conducted under quasi-static loading assumptions and does not simulate dynamic, real-time operational conditions like vibration or irregular wave impact. The importance of such dynamic effects is underscored by Ariesta et al. [17], who found that transient wave loads can notably accelerate fatigue crack growth in marine panels. Finally, the fatigue life estimation in this study is based on a deterministic application of Paris' Law, assuming uniform load cycles. This excludes the influence of stochastic loading conditions, which are captured in probabilistic fatigue models like those applied by Wu & Ni [26]. These limitations provide important context for interpreting the findings and highlight directions for future research aimed at improving the realism and comprehensiveness of crack propagation analysis in ship sandwich constructions.

2.2 Material properties and structure model

The materials used in sandwich structures play a crucial role in the overall performance of ship components. This study focuses on a steel-based hybrid sandwich structure, using steel as the face sheets and polyurethane elastomer as the core. Sandwich materials are widely adopted in shipbuilding for their high strength-to-weight ratio and weight reduction benefits. These structures consist of a lightweight core such as foam, balsa, or polyurethane bonded between strong outer layers like composites or metals [27]. This configuration improves fuel efficiency, increases payload capacity, and enhances overall ship performance without compromising structural integrity [28]. The material properties are summarized in Table 1 and visualized in Figure 2.

Material properties, such as Young's modulus and density, significantly influence crack propagation behavior [29]. Higher Poisson's ratio generally indicates increased material resistance to crack initiation and propagation, as it reflects the material's ability to undergo lateral deformation under axial stress [30]. In some cases, cracks may stop or change direction when they encounter areas with different material properties, highlighting the complex interaction between material

Table 1 Material Properties of the Sandwich Structure

No	Part	Material	Density (kg/m ³)	Young 'Modulus (MPa)	Poisson Ratio
1	Face/Bottom Plate	ASTM A36 Steel	7850	2,6x10 ⁷	0,3
2	Core	Polyurethane Elastomer	1124	387	0,36

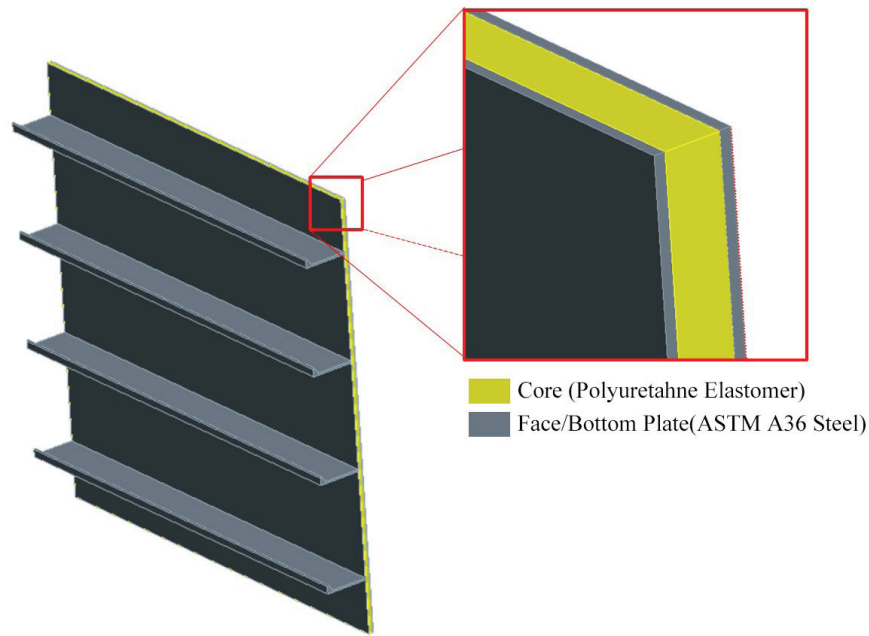


Figure 2 Sandwich material illustration applied in ship side structure

properties and crack growth [31]. The sandwich material is applied to the side structure of a 17500 DWT tanker ship. The principal dimensions of the ship are written in Table 2.

Z-rule or equivalent section modulus of the ship is essential for determining the appropriate thickness for the application of sandwich material on the ship’s hull sides. The equivalent section modulus is 18,808,332.18 cm³ [7]. After calculation, the thickness of the sandwich material in this study is detailed in Table 3.

Initial crack sizes of 25 mm, 50 mm, and 75 mm were applied at the center of the sandwich plate core,

Table 2 Principal dimension of 17500 DWT tanker

Length Overall	157,5 m
Length Perpendicular	149,5 m
Breadth	27,7 m
Height	12 m
Draught	7 m

simulating damage from compressive loads during ship operation [32]. This location also allows for clearer analysis of crack propagation direction [33]. Figures 3 illustrate the crack position.

Table 3 Face/bottom plate and core thickness

Variation	Face Plate Thickness (mm)	Core Thickness (mm)	Variation	Face Plate Thickness (mm)	Core Thickness (mm)
SA-C1	4	15	SB-C1	6	15
SA-C2		18	SB-C2		18
SA-C3		21	SB-C3		21
SA-C4		24	SB-C4		24



Figure 3 Initial crack and plate model illustration on this study

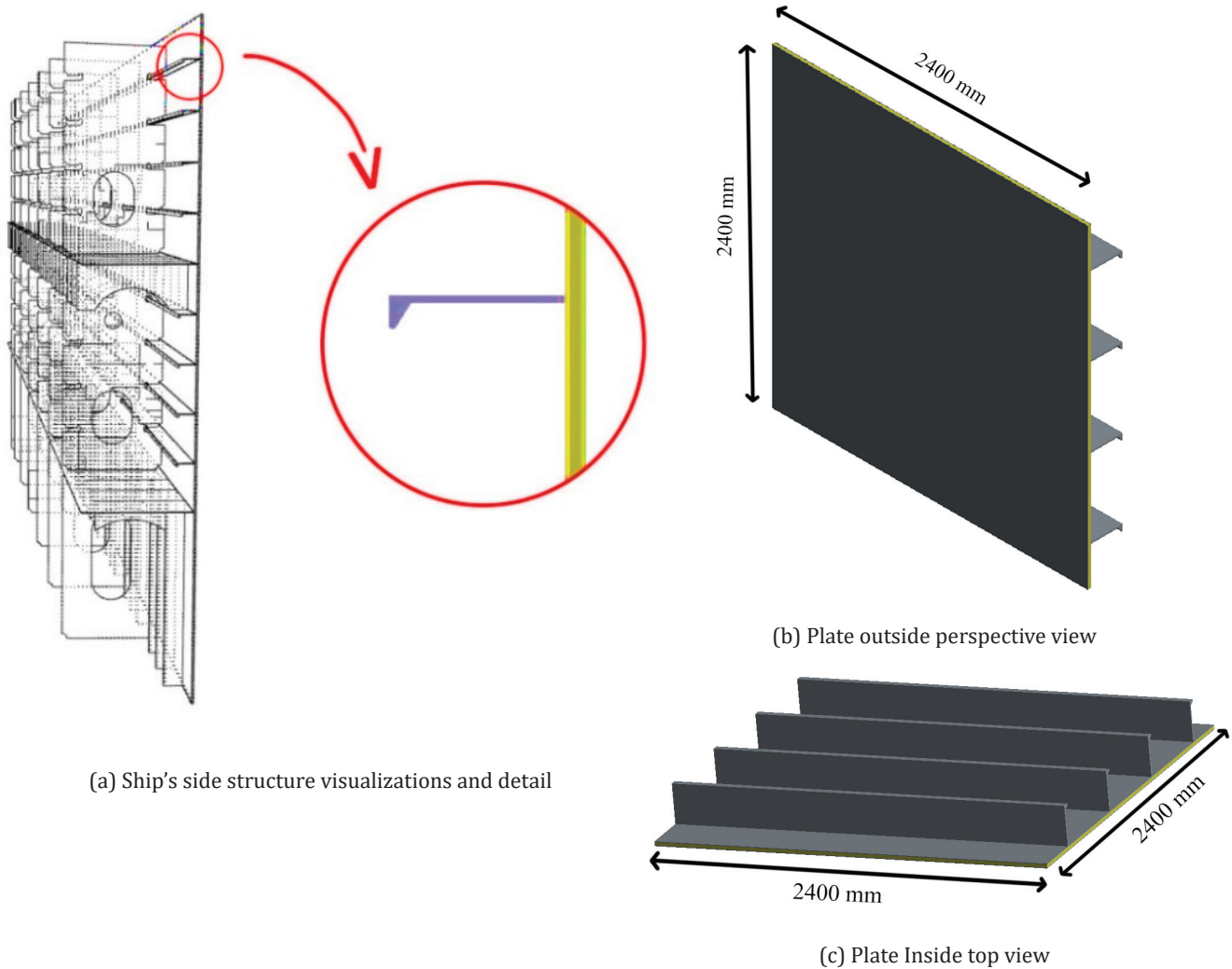


Figure 4 Sandwich plate dimension and structure visualization

The structural model used in this study was designed to imitate the actual configuration of a ship's side hull plating, illustrated in Figure 4(a)-(c). A representative plate panel was selected for analysis, focusing on the area subjected to the most significant operational loads, particularly from lateral wave pressure. This approach allows for an accurate simulation of stress conditions experienced in service.

2.3 Operational Load

A thorough load analysis is essential to define the structural requirements of a ship. These include static loads (e.g., still water, buoyancy, self-weight), quasi-static loads from hydrostatic pressure variations due to wave and ship motion, and dynamic loads such as

wave impacts on the ship's side [34]. For this study, the fracture analysis focused on the core of the sandwich structure, evaluating maximum load effects across various thickness configurations. Since the core doesn't directly absorb sea loads, but receives them through surrounding plates and profiles, a separate numerical analysis was conducted. This simulation distributed the loads across the sandwich plate to determine the resulting von Mises stress in the core.

The corresponding force was then calculated using stress-area relations, with the load setup illustrated in Figure 5. Based on classification standards, the maximum applied load was estimated at $110,608 \text{ kN/m}^2$, representing the highest hydrostatic and hydrodynamic forces on one side of the ship [35], as summarized in Table 4.

Table 4 The load on the core in each structure variation

Variation	Face thickness (mm)	Core thickness (mm)	Core's Load (MPa)	Variation	Face thickness (mm)	Core thickness (mm)	Core's Load (MPa)
SA-C1	4	15	0,1057	SB-C1	6	15	0,1073
SA-C2		18	0,0969	SB-C2		18	0,0973
SA-C3		21	0,0867	SB-C3		21	0,0888
SA-C4		24	0,0777	SB-C4		24	0,0824

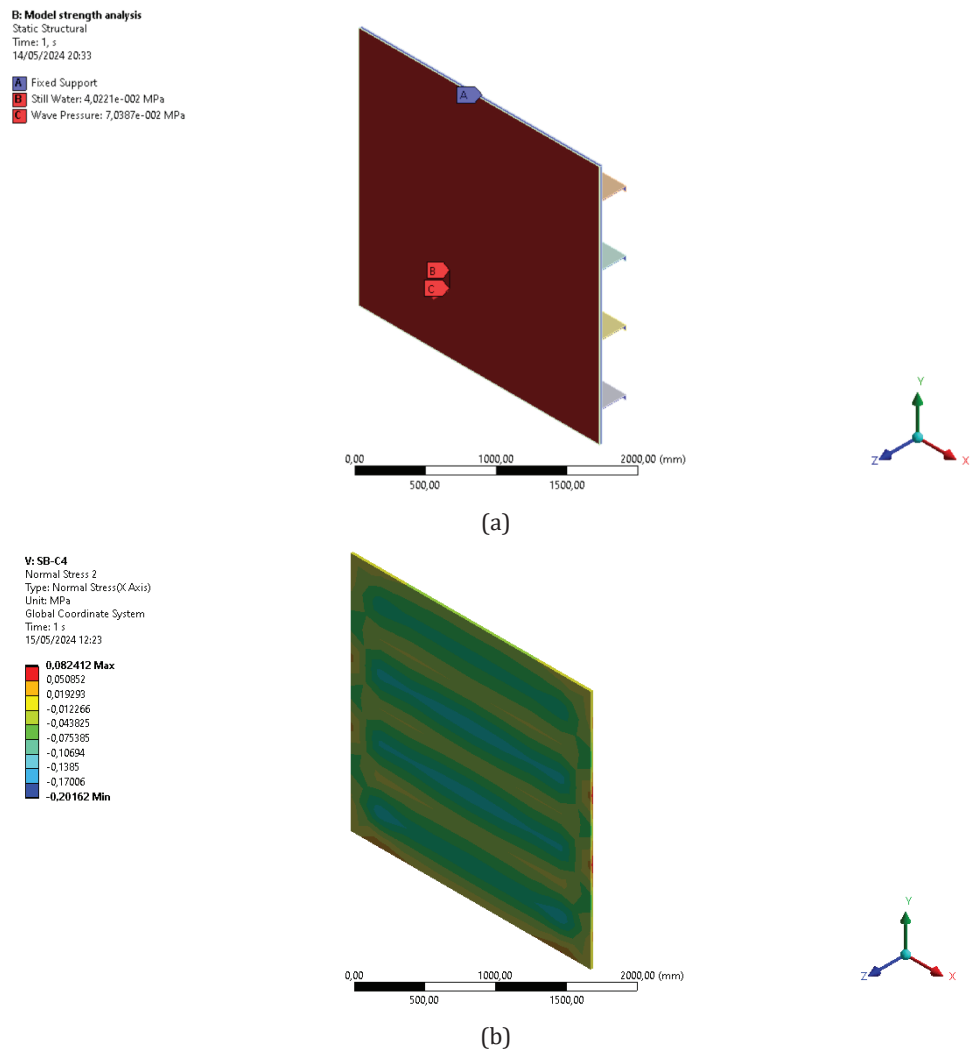


Figure 5 Load analysis configuration (a) FEM Configuration & (b) Load distribution on the core

3 Crack Growth Numerical Modeling

3.1 Crack Growth and Strength Reduction Analysis

Material toughness characteristics to prevent cracking are used to simulate the propagation in the study. The growth rate can be determined through the stress intensity factor range function, based on the Paris-Erdogan equation, also known as Paris' Law, which can be defined in Equation 1:

$$\frac{da}{dN} = C \Delta K^m \tag{1}$$

With da/dN representing the crack propagation rate, ΔK is the Stress Intensity Factor Range, and C and m are coefficients specific to each material [36]. These coefficients are obtained by performing regression on experimental test results [37]. The results of regression analysis form the basis for determining the Paris Law coefficients. These coefficients, when integrated into the Paris Law

equation, enable the prediction of crack growth rates under various operational conditions. Additionally, the Paris Law has been analyzed in prior research by Syahab et al [38], which the experimental results converged to constant values of $C = 1.68E-6$ and $m = 0.56$.

The strength reduction factor is a parameter used in structural reliability analysis to account for the reduction in strength that occurs due to uncertainties in design and material factors. This factor is used to reduce the nominal strength of the structure calculated to consider the variations and uncertainties present. This factor depends on the type and level of uncertainty in the specific structural analysis. Generally, the strength reduction factor has a value between 0 and 1, where a value of 1 indicates low uncertainty or a high level of confidence in the calculated strength, while a lower value indicates a higher level of uncertainty. This strength reduction is performed to avoid the risk of undesirable structural failure and to ensure that the calculated strength is conservative in considering the existing uncertainties. By reducing the calculated strength of the structure, the strength reduction factor ensures that the structure has adequate safety factors when subjected to working loads [39, 40]. This factor, which can be denoted as R , is obtained using equations 2 & 3:

$$R_p = \frac{\sigma_{ex}}{\sigma_r} \quad (2)$$

$$R_{al} = \frac{\sigma_{ex}}{\sigma_{max}} \quad (3)$$

Equation 2 represents the strength reduction factor, with σ_r being the stress that occurs in the structure during damage. Meanwhile, Equation 3 is the allowable factor, with σ_{max} being the stress of the damaged structure during failure. Both aspects will be compared with the stress of the structure under normal conditions. The fatigue life can be estimated after determining the number of cycles for each crack size that occurs. The calculation of cycles until reaching final crack propagation is used to determine crack growth. The life of the structure can be calculated using the Plagmern formula approach, where the sought factor is the fatigue life at that structural detail. Equation 4 & 5 is obtained to estimate the fatigue life by inputting the crack cycle values to understand the fatigue process as applied in Leheta et al's study [41], with T as the fatigue life, N is the cycle, and L is the ship length.

$$T = \frac{4 \log L}{a_0} N \text{ (in seconds)} \quad (4)$$

$$T = 1.492 \times 10^{-7} \log L \times N \text{ (in years)} \quad (5)$$

3.2 Numerical Model

Numerical simulation, particularly Finite Element Analysis (FEA), is widely used to study complex structural behavior that is difficult to replicate experimentally. Element size is selected based on prior experience to capture stress concentrations, especially near openings and applied loads, with accuracy depending on mesh refinement [42]. The SMART (Separating Morphing and Adaptive Remeshing Technology) method automatically updates the mesh near the crack tip at each solution step, offering better scalability and eliminating the need for custom elements [43]. In this study, SMART method executed using ANSYS feature. SMART uses unstructured tetrahedral meshes that adapt to crack growth, significantly reducing preprocessing and computation time [44, 45]. Crack direction is determined using the Maximum Tangential Stress (MTS) criterion, which states that cracks propagate in the direction of maximum tangential stress near the crack tip. Stress and the corresponding Stress Intensity Factor (SIF) are calculated using Eq. 6 and 7 [43, 46].

$$\sigma_{\theta\theta} = \frac{1}{\sqrt{2\pi r}} \cos\left(\frac{\theta}{2}\right) \left(K_I \cos^2\left(\frac{\theta}{2}\right) - \frac{3}{2} K_{II} \sin(\theta) \right) \quad (6)$$

$$K_{eq} = \cos\left(\frac{\theta_0}{2}\right) \left[K_I \cos^2\left(\frac{\theta_0}{2}\right) - \frac{3}{2} K_{II} \sin(\theta) \right] \quad (7)$$

Asymmetric meshes can lead to inaccuracies in the calculation of the SIF. By ensuring that the elements around the crack tip are balanced and evenly distributed. Symmetric mesh facilitates the accurate determination of the turning angle and the crack growth direction as predicted by the MTS criterion. The illustration of UMM geometry in Figure 6(a) helps in understanding the movement of the finer mesh as it follows the crack tip growth along the fracture propagation path. In this analysis, the finite element method configuration has been set up to simulate fractures in ship plate structures, with the mesh result displayed in Figure 6(b) for global mesh, and 6(c) for finer mesh around crack tip. The necessary fracture properties have been input into the FEM software, including the Paris Law coefficients used to predict the crack propagation rate. The Patch Conforming method is used as part of the UMM in SMART Crack Growth analysis. A finer mesh is utilized around the crack tip to enhance the accuracy of the simulation in this critical area.

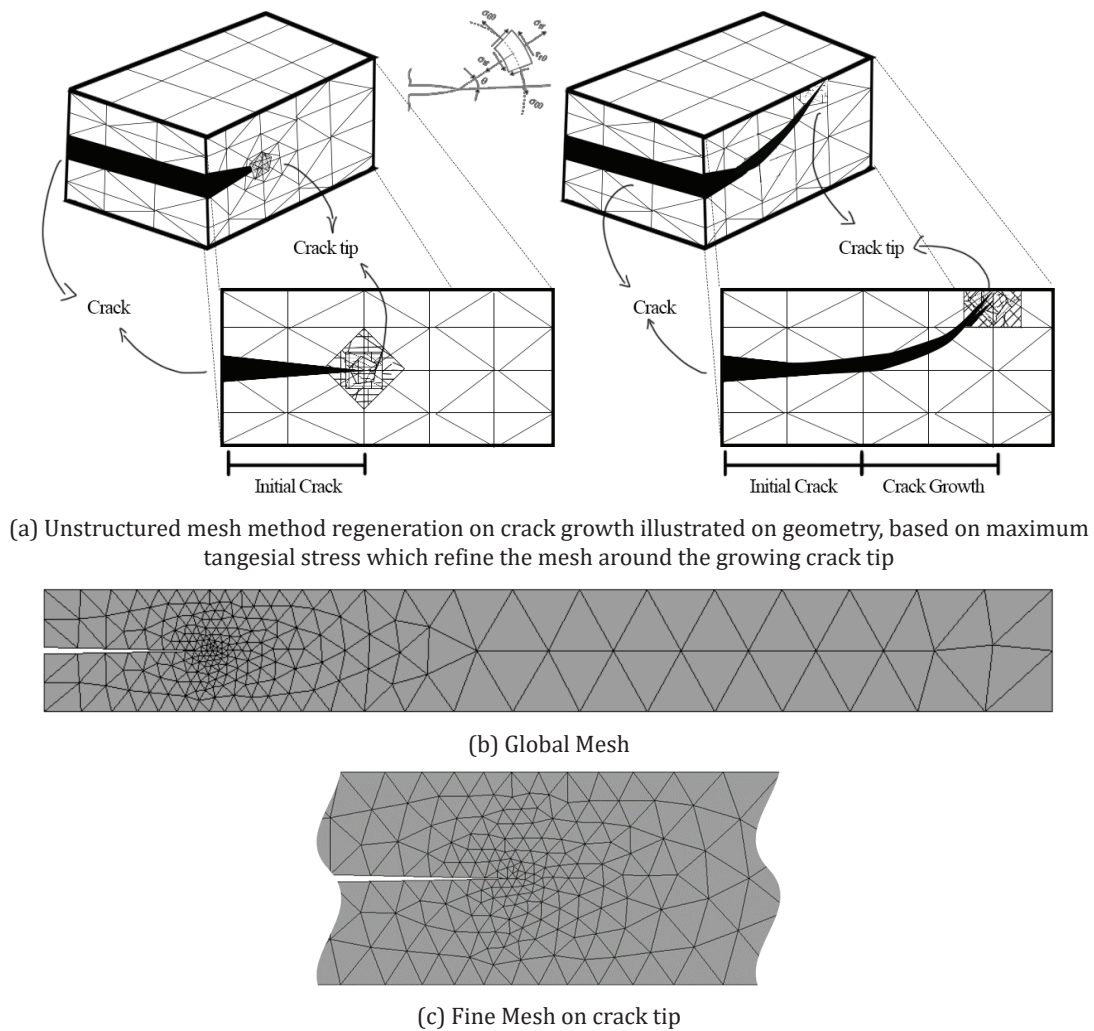


Figure 6 Illustration of the mesh simulation model with finer mesh on the crack tip

4 Result and Discussions

4.1 Material Validation

The accuracy level in the finite element analysis process is directly proportional to the increasing number of elements used. However, the increase in the number of elements also affects the time and cost required during the analysis process [47]. Material behavior was validated through experimental testing, using a modified JIS K7086 method to assess mode II (shear/in-plane) damage, as outlined by Siswanti et al. [48]. Figure 7(a) shows the test setup, while Figure 7(b) presents the corresponding numerical model.

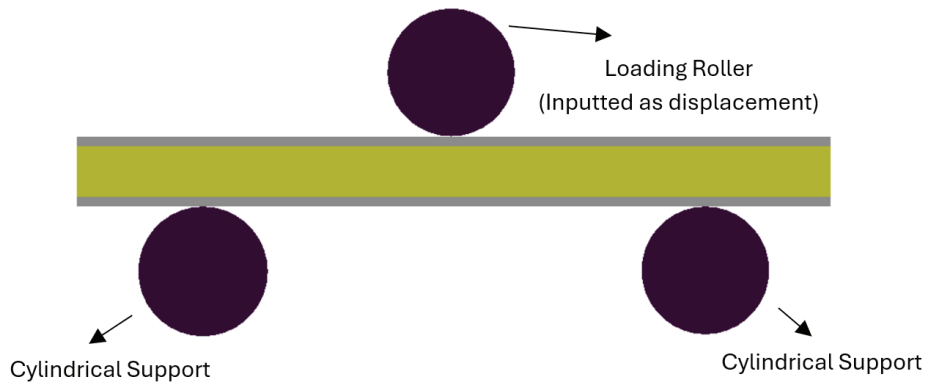
The numerical simulation was refined through adjustments in mesh size, time steps, and validated by comparing results with experimental data as shown in Figure 8. Despite minor discrepancies due to unmodeled phenomena like core fracture and delamination, overall agreement confirmed the model's behavior accuracy [49, 50]. A convergence study, shown in Figure 7 and Table 5, identified a medium mesh size as optimal—achieving accuracy within 6% of experimental results while maintaining computational efficiency. This setup ensures a stable basis for further crack propagation analysis [51].

Table 5 Convergency study result comparison

Mesh size (mm)	Coarse	Medium	Fine	Finest
Ultimate stress (MPa)	19,7080	18,6020	18,6040	18,8470
Element	156	226	253	308
Comparison	-	5,61%	0,01%	1,30%



(a) Experimental test



(b) Numerical setup

Figure 7 Sandwich material bending test

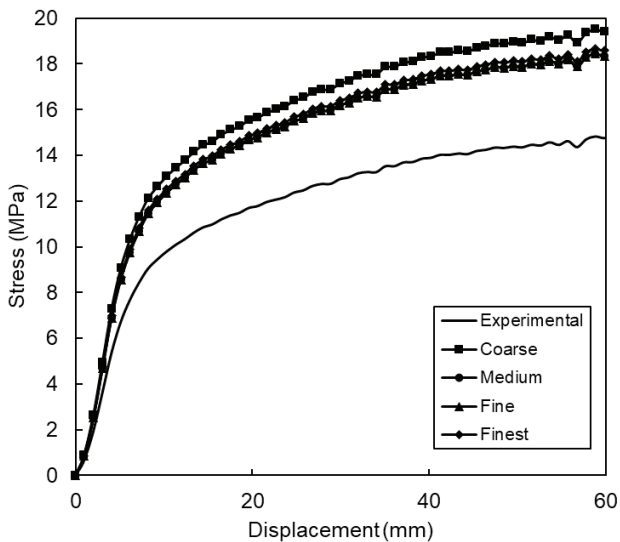


Figure 8 Comparison for numerical and experiment analysis

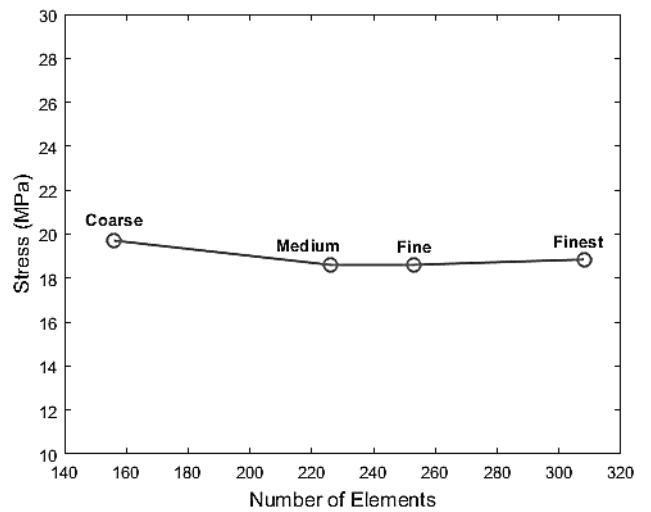


Figure 9 Convergency study for numerical analysis of the material behavior

4.2 Crack Simulation

In the simulation configuration, boundary conditions were applied to replicate the integration of the ship’s side structure with adjacent components. To represent the effect of welded joints that connected each plate at side structure, all edges of the sandwich plate model were fully fixed. This setup simulates the constraints imposed by surrounding structural elements, thereby reflecting the actual support conditions encountered in service. The applied loading was configured to simulate a beam sea condition, where wave action impacts the ship laterally and induces significant stress on the side plating. In practice, ship hull structures are subjected to fluctuating ten-

sile and compressive stresses due to the irregular and dynamic nature of wave loading [52]. Rather than applying a compressive load on the outer faceplate, the simulation applied a tensile force from the inner surface, mimicking the internal stress response caused by hull flexure during wave encounters. This configuration was intentionally selected to promote crack propagation within the sandwich core and to more accurately capture the tensile stress patterns that can emerge under operational deformation scenarios. Boundary condition for crack simulation is illustrated in Figure 10.

Damage analysis was validated through a comparison on each mesh size variations, as shown in Figure 11.

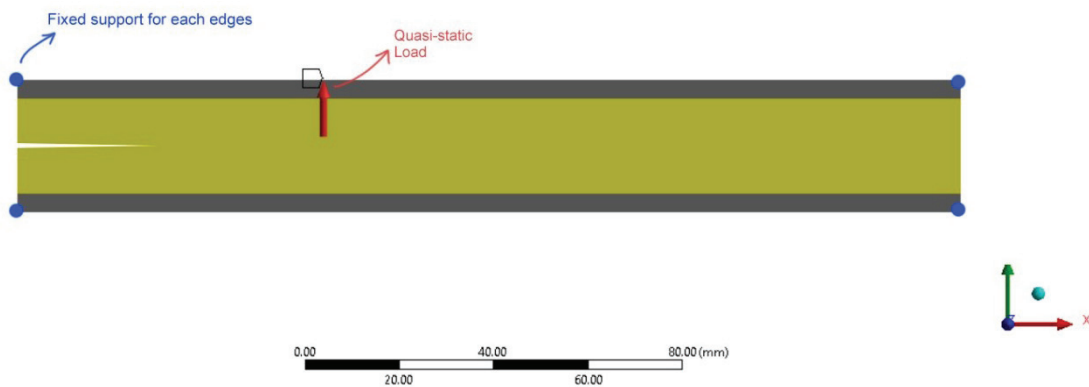


Figure 10 Boundary condition and load assumptions for mesh configurations illustrated with model using interface plate

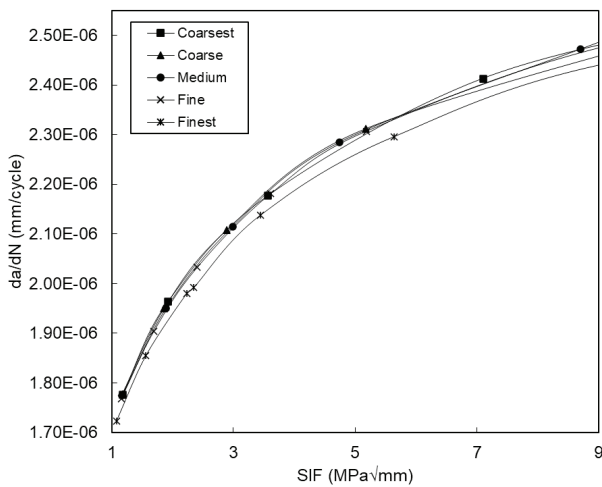


Figure 11 Comparison of each mesh size results on fracture simulation

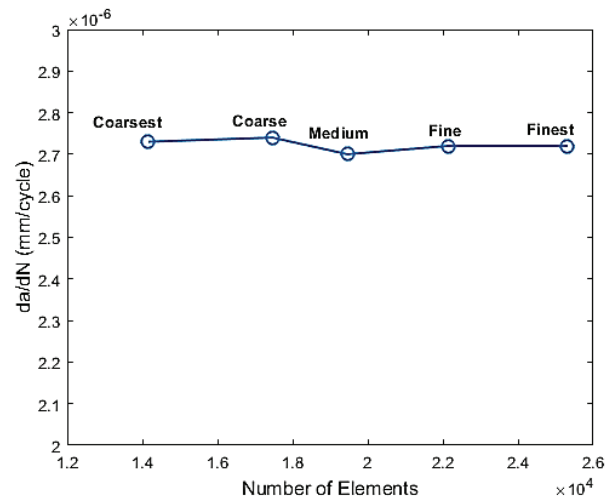


Figure 12 Convergence study of fracture simulation

Table 6 Comparison of every fracture simulation’s mesh size

Global Size (mm)	Coarsest	Coarse	Medium	Fine	Finest
Element	14159	17460	19458	22135	25319
da/dN	2,73E-06	2,74E-06	2,70E-06	2,72E-06	2,72E-06
Comparison	-	0,32%	1,46%	0,67%	0,19%

The assessment, based on SIF values and crack propagation speed, showed minimal differences across mesh sizes, indicating accurate material response under loading conditions. This is further supported by the convergence study in Table 6 and Figure 12, where value differences between mesh sizes were below 1.5%. The results confirmed that a medium mesh size achieved convergence, offering an efficient meshing process that reduces computational time without compromising analysis quality. Therefore, the medium mesh size was selected for the simulation to ensure high validity of the analysis. Result from this validation used in mesh setup and refinement utilized in this study are visualized in Figure 13, showed in each propagation progress with green line illustrated the crack growth size.

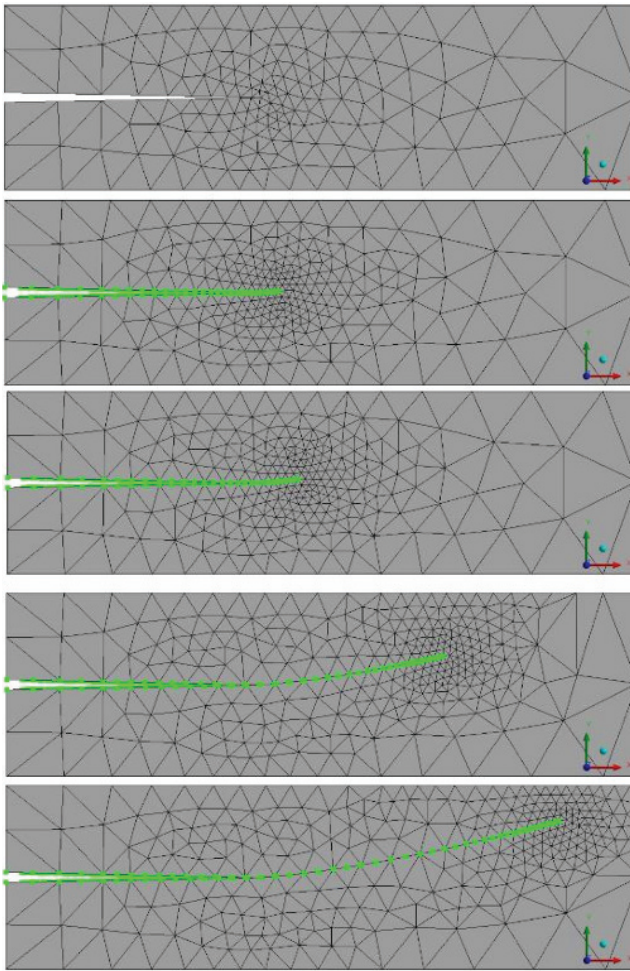


Figure 13 Mesh refining for material's crack growth using medium mesh size

Damage analysis was performed on structure materials to examine crack propagation direction and growth rate under varying conditions, including face/bottom plate thickness, core thickness, and initial crack length. The study covered face/bottom plates of 4 mm and 6 mm, core thicknesses from 15 mm to 24 mm, and initial crack lengths of 25 mm, 50 mm, and 75 mm. The results, including Stress Intensity Factor (SIF), crack extension, load cycles, and propagation rate (da/dN), show that crack behavior follows similar patterns across variations [53]. Figure 14 illustrates crack propagation properties. The analysis aligns with the Paris-Erdogan theorem, showing an initial phase of slow crack growth, followed by a rapid increase in propagation rate as the crack extends.

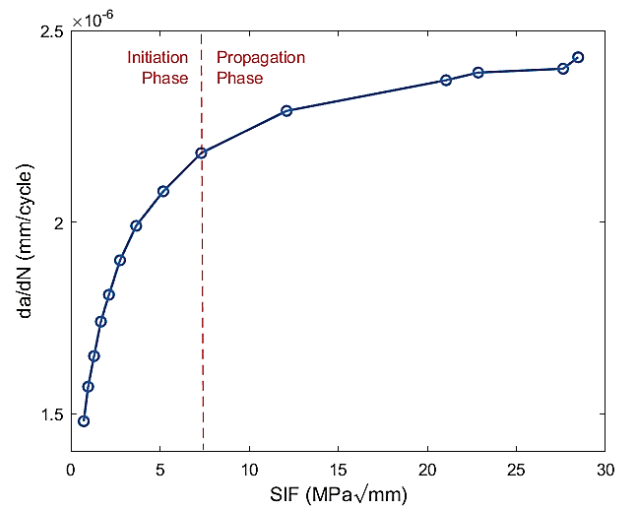


Figure 14 Propagation behavior on structure

After reaching its peak rate, the crack enters a stable phase where growth continues at a constant rate, influenced by material properties and stress conditions. Crack propagation in the structures, shown in Figure 15, follows a pattern aligned with the applied wave loading. Cracks generally propagate inward, following the load path, as the stresses from the wave loading direct the crack toward the most stressed areas. In the observed images, cracks often halt at the interface between the face/bottom plate and the core. This occurs due to the difference in mechanical properties between the materials, where the crack's progression is influenced by the strength of the interfacial bond and stress distribution at the interface [54].

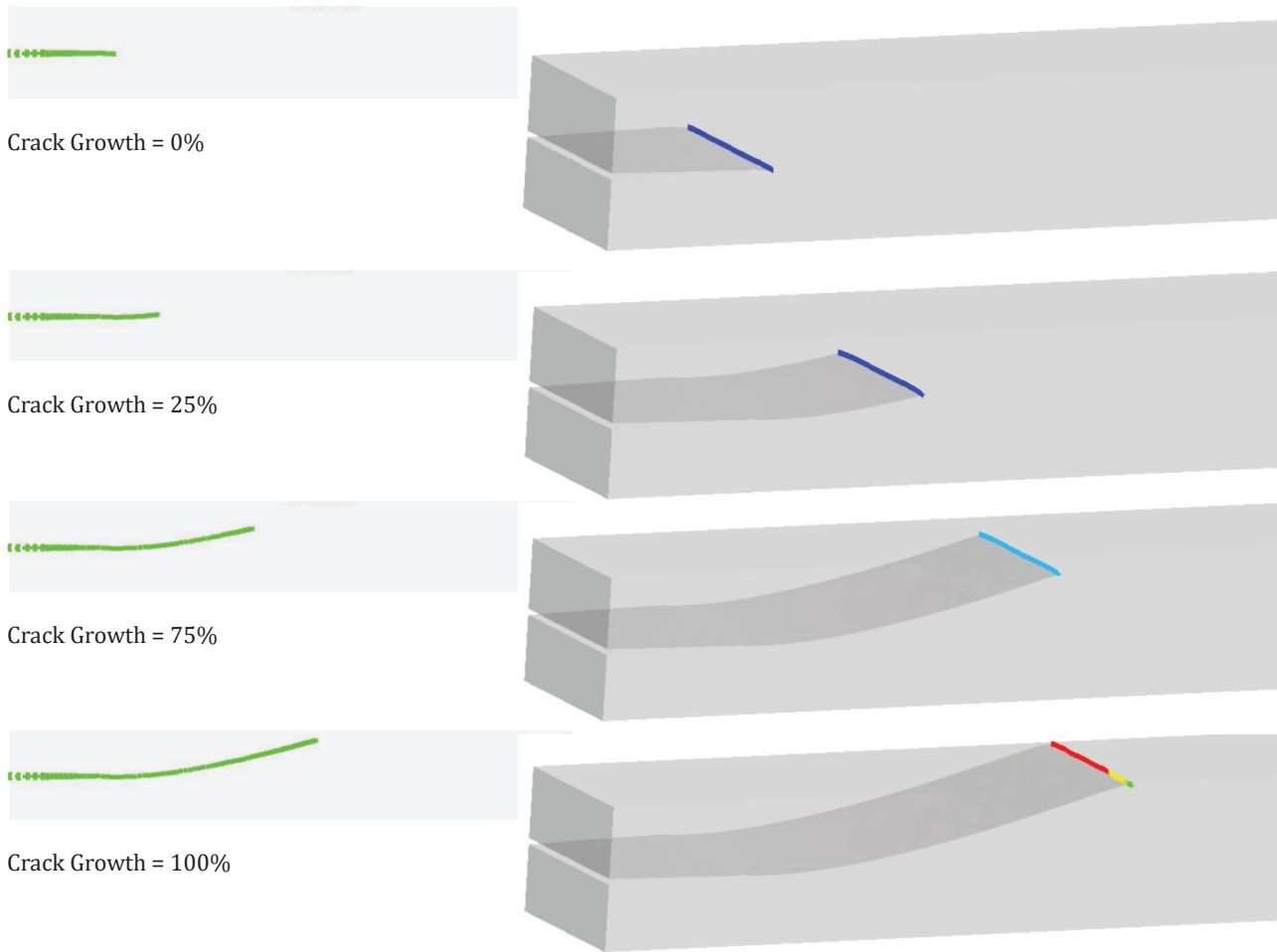


Figure 15 Crack propagation visualization on structure core

4.3. Structure Variations Effect to Crack Propagation

4.3.1 Comparison of damage for each variation in the thickness of the face/bottom plate

A comparison of sandwich structures with different face/bottom plate thicknesses was conducted using two models with the same core thickness but varying plate thicknesses, as shown in Figure 16. The results reveal that, in the early phase, crack propagation responses are nearly identical for both variations. The SIF values differ by 5.70%, with the 6 mm thickness having a higher value. The 6 mm plate requires approximately 1.99% more cycles than the 4 mm plate to initiate crack propagation, indicating that plate thickness affects the number of cycles needed. At the maximum propagation point, the 4 mm plate has an SIF 2.38% smaller than the 6 mm plate, showing that thicker plates can better withstand stress. The crack extension points for both variations are nearly identical, with only a 0.02% difference. Figure 17 shows that although crack growth direction is similar, the main differences lie in stress intensity and crack propagation rate. Thicker plates delay crack

growth, requiring more load to induce cracks and slowing propagation rates, which also concluded in Zhou and He [55] research.

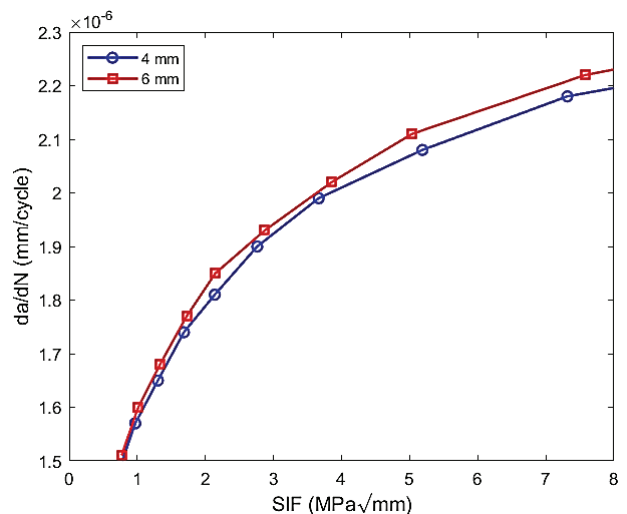


Figure 16 Comparison of crack propagation with plate thickness variations

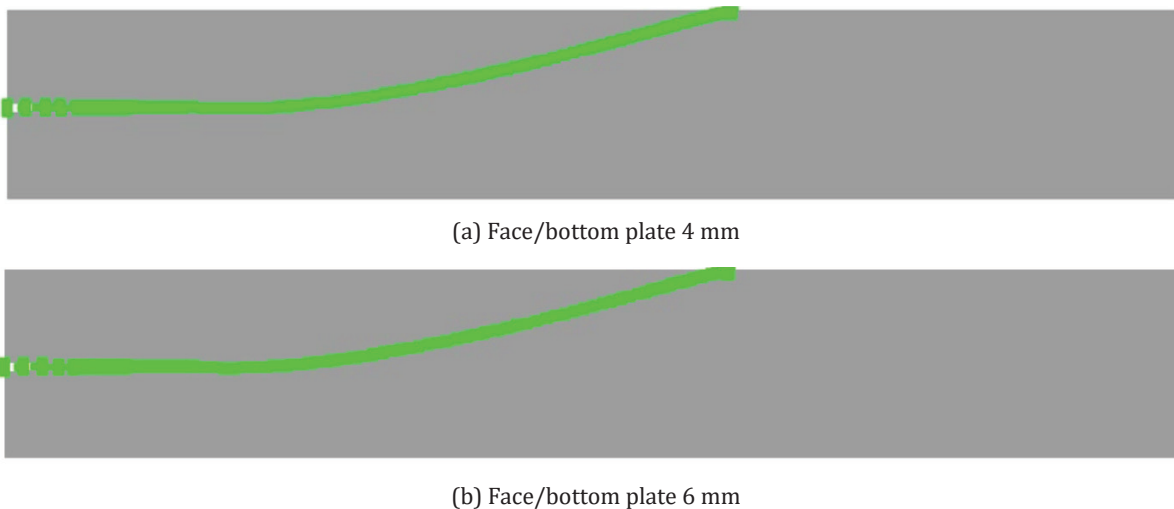


Figure 17 Comparison of crack propagation visualization on different face/bottom plates

4.3.2 Comparison of damage for each variation of core thickness

Comparison of sandwich structures with varying core thicknesses used four models with the same face/bottom plate thickness and initial cracks but different core thicknesses. The results, shown in Figure 18, reveal that thinner cores lead to faster crack propagation.

In the SA-25 case, with an initial crack of 25 mm, the 15 mm core (SA-C1) exhibited the highest crack growth rate across all stress intensity factor (SIF) values. As core thickness increased to 18 mm (SA-C2), 21 mm (SA-C3), and 24 mm (SA-C4), the propagation rate decreased progressively. This indicates that even with a relatively small initial crack, a thicker core substantially reduces crack growth, likely due to improved energy absorption and stiffness. The separation between the curves becomes more visible at higher SIF levels, suggesting that the influence of core thickness becomes more critical under increased loading. In SA-50, where the initial crack length increases to 50 mm, the differences between the models become more pronounced. SA-C1 (15 mm core) again shows the fastest propagation, while SA-C4 (24 mm core) shows the slowest. The propagation rates of the 18 mm (SA-C2) and 21 mm (SA-C3) cores fall between these two extremes, displaying a consistent gradient. This reinforces the notion that thicker cores are more effective in resisting crack growth, especially as the extent of initial damage increases. SA-75 presents the case with the largest initial crack length, and the effect of core thickness is most evident here. The 15 mm core model (SA-C1) shows a sharp rise in crack growth rate, while the 24 mm core (SA-C4) maintains significantly lower values. Once again, the intermediate core thicknesses (18 mm and 21 mm) display proportional behavior. This indicates that the structural advantage of using

thicker cores becomes increasingly important as both initial damage and stress levels rise.

Similar trends are observed in the SB series, which features thicker face and bottom plates. In SB-25, the 15 mm core (SB-C1) results in the highest crack propagation rate, while the 24 mm core (SB-C4) slows the crack growth most effectively. However, the overall propagation rates in SB-25 are slightly lower than their SA counterparts, likely due to the additional stiffness provided by the thicker outer plates. The 18 mm (SB-C2) and 21 mm (SB-C3) models again follow a clear intermediate path between the two extremes. In SB-50, the crack propagation curves diverge further, with SB-C1 (15 mm core) accelerating faster than all other models. The 24 mm core (SB-C4) maintains the lowest propagation rate across the full SIF range, while SB-C2 and SB-C3 demonstrate moderate reductions. These differences grow more noticeable at higher SIF values, emphasizing how both faceplate thickness and core thickness contribute to overall fatigue resistance. In the SB-75 case, the trend remains consistent. The 15 mm core (SB-C1) exhibits the steepest increase in crack growth rate, while the 24 mm core (SB-C4) once again demonstrates the slowest propagation. The intermediate core thicknesses maintain their respective positions, highlighting the progressive improvement in damage tolerance with increasing core thickness.

Overall, the results confirm that increasing core thickness from 15 mm to 24 mm significantly enhances resistance to crack propagation in both plate configurations and across all initial crack lengths. The maximum observed reduction in propagation rate reached approximately 28%, with an average reduction of 8% across all variations. Additionally, crack extension was found to be longer in thicker-core structures, with a maximum difference of 54% in final crack length between the 15 mm and 24 mm cores, and an average increase of about 30%.

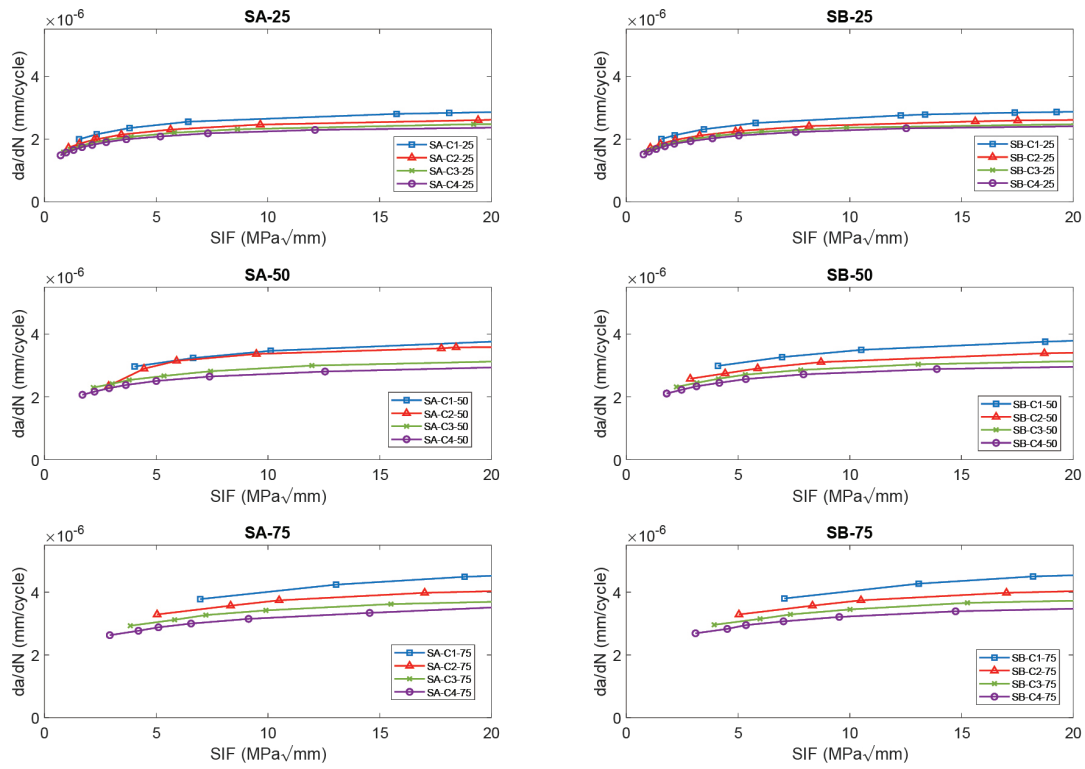


Figure 18 Comparison of crack propagation in structures with variations in core thickness

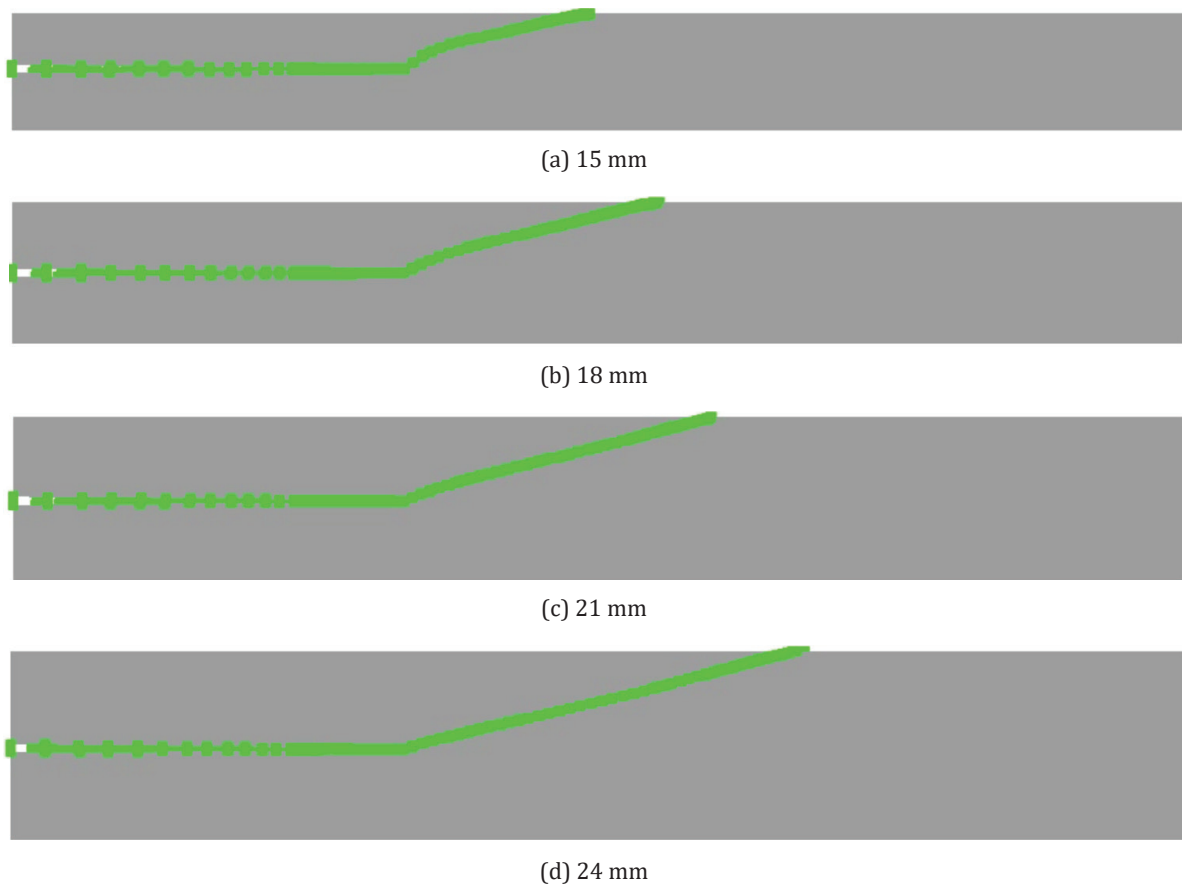


Figure 19 Comparison of the visualization of crack with varying core thicknesses

Variations in faceplate thickness have a minimal effect on propagation behavior. The comparison is clearly shown in the crack visualizations in Figure 19. In all variations, cracks propagate inward, following the load direction from the wave forces. The crack length varies with the structure’s thickness, with shorter cracks observed in the 15 mm plate core compared to those in thicker plates. Thicker plates result in slower crack propagation and longer crack extensions. These findings align with Dhaliwal and Newaz [18], who showed that increasing core thickness enhances durability and load capacity, contributing to slower crack propagation and longer extensions.

4.3.3 Comparison of damage for each variation in initial crack size

The comparison of model variations with different initial crack sizes is shown in Figure 20.

Figure 20 presents the comparison of crack propagation behavior in sandwich structures with different initial crack lengths across varying core thicknesses and plate configurations. Each subplot represents a different core thickness: 15 mm (C1), 18 mm (C2), 21 mm (C3), and 24 mm (C4), under two structural setups: SA with thinner face/bottom plates (left column) and SB with thicker face/bottom plates (right column). Within each plot, the initial crack length is varied (25 mm, 50 mm, and 75 mm), and the results consistently demonstrate that larger initial cracks lead to faster propagation rates across all configurations. In the SA-C1 chart, which features a core thickness of 15 mm with thin faceplates, the propagation rate increases noticeably with initial crack size. The 75 mm initial crack (SA-C1-75) produces the highest propagation rate, followed by the 50 mm (SA-C1-50), and finally the 25 mm crack (SA-C1-25), which propagates the slowest. The wide gap between the curves illustrates the sensitivity of this thin-core config-

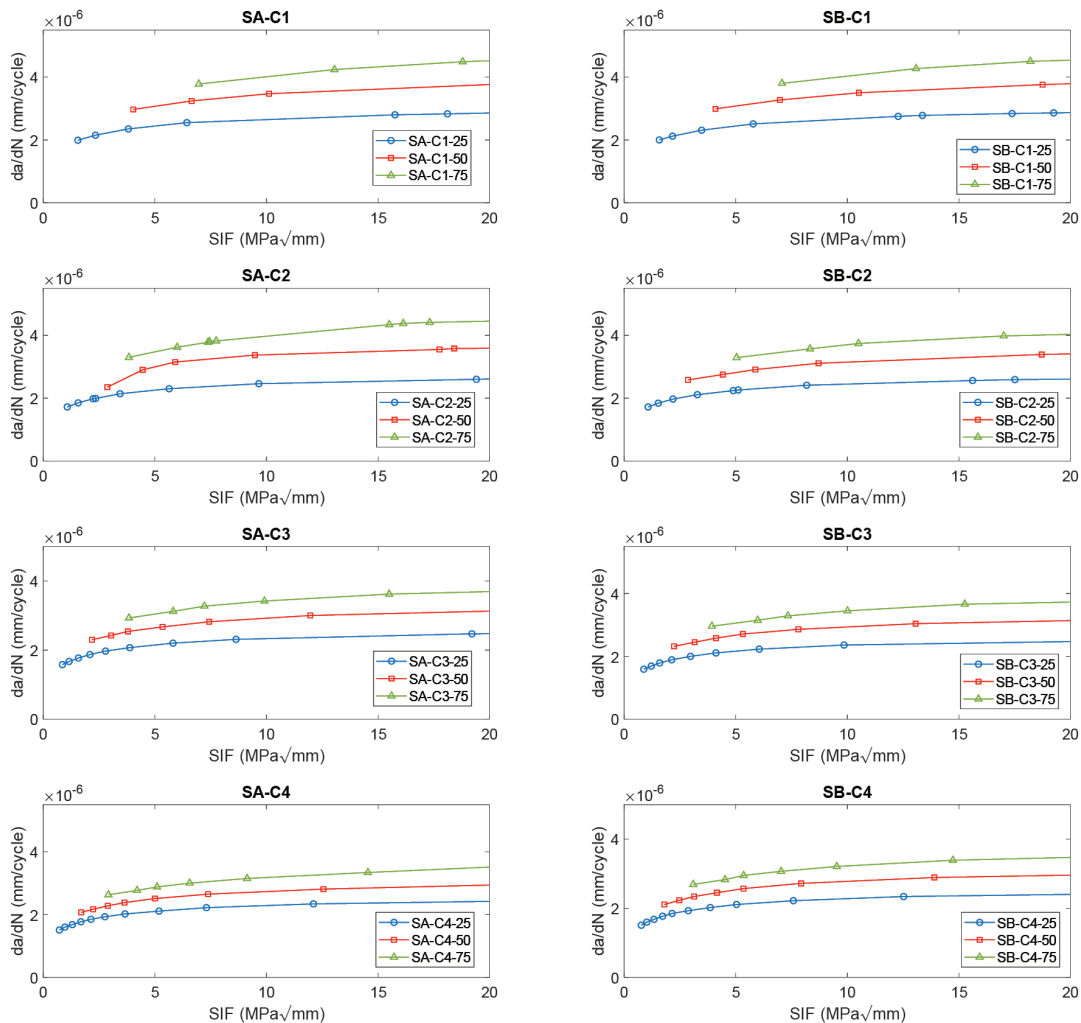


Figure 20 Comparison of crack propagation in sandwich structure with variations in initial crack size.

uration to initial crack size, with higher stress intensity factors (SIF) associated with longer cracks accelerating crack growth significantly. A similar pattern is evident in SA-C2, which has a slightly thicker 18 mm core. Although the overall propagation rates are marginally lower than in SA-C1, the trend remains unchanged: the longer the initial crack, the faster the propagation. The SA-C2-75 model continues to show the steepest crack growth, indicating that even a modest increase in core thickness does not fully compensate for the elevated stress concentration induced by longer cracks. In the SA-C3 subplot, with a 21 mm core, the spacing between propagation curves remains visible but slightly reduced compared to thinner cores. While SA-C3-75 still displays the highest propagation rate, the difference between it and the 50 mm or 25 mm crack models is narrower, suggesting improved resistance due to increased core thickness. This highlights the influence of core thickness in mitigating the acceleration of crack growth, especially in panels with large initial flaws. SA-C4, with the thickest core at 24 mm, further demonstrates this behavior. The curves for 25 mm, 50 mm, and 75 mm initial cracks are closer together compared to the previous subplots. Although the 75 mm crack still propagates faster, the rate difference between all three initial crack lengths is reduced. This indicates that increasing the core thickness effectively suppresses the crack driving force, even when the initial crack is relatively large.

Turning to the SB series, where face and bottom plates are thicker, similar trends are observed. In SB-C1 (15 mm core), the 75 mm crack shows the highest propagation rate, while the 25 mm crack remains the lowest. However, all curves lie slightly below their SA-C1 counterparts, suggesting that the increased faceplate stiff-

ness in the SB configuration slightly reduces crack growth across all initial crack lengths. The SB-C2 chart mirrors this behavior. The ranking of propagation rates remains the same, namely, SB-C2-75 being the fastest, followed by SB-C2-50 and SB-C2-25. However, the overall gap between curves is slightly smaller than in SB-C1. This suggests a compounded effect: both increased core thickness and stiffer outer plates help suppress crack propagation. In SB-C3, with a 21 mm core, the propagation curves tighten further. Although SB-C3-75 still leads in crack growth rate, the difference from SB-C3-50 and SB-C3-25 diminishes further. This reinforces the conclusion that thicker cores and faceplates work together to slow down crack advancement, particularly when stress concentrations are elevated due to large initial cracks. Finally, in SB-C4, which combines the thickest core and faceplates, the influence of initial crack size is still apparent but considerably reduced. The propagation rate for the 75 mm initial crack remains higher than the others, but the overall growth rate is the lowest among all subplots in the figure. This configuration demonstrates the most effective resistance to crack growth, confirming that a combination of thick cores and robust faceplates offers the best defense against fatigue failure, especially when initial damage is already present.

Figure 21 illustrates the visualization of crack propagation in sandwich plate structures with varying initial crack sizes. As shown, the crack path becomes increasingly extended and advances further through the core as the initial crack length increases from 25 mm to 75 mm. The 25 mm crack (Figure 21a) exhibits a relatively short and curved propagation path, while the 50 mm crack (Figure 21b) shows a longer, more linear growth. In the case of the 75 mm initial crack (Figure 21c), the propa-

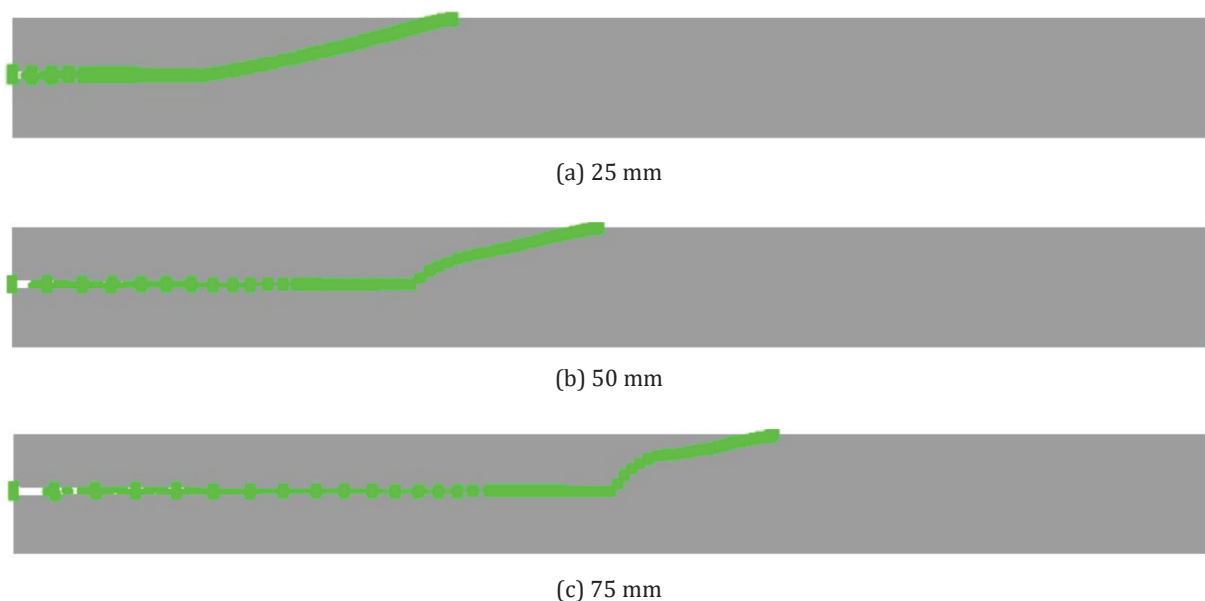


Figure 21 Visualization of crack propagation in sandwich plate structure with variations in initial crack size

gation is both longer and more aggressive, indicating that larger initial flaws lead to significantly faster and more extensive crack growth. This visualization supports the numerical results, confirming that longer initial cracks generate higher stress intensity and promote earlier failure in the sandwich structure.

Across all configurations, the results confirm that larger initial cracks consistently produce faster propagation due to higher SIF values and localized stress concentrations. On average, the propagation rate increases by approximately 73% when comparing 25 mm and 75 mm cracks, which is consistent with the expected behavior in fracture mechanics. While core thickness has a clear and significant impact variations in faceplate thickness show only a modest effect by comparison. Consequently, larger initial cracks lead to faster crack propagation and shorter extension lengths, indicating quicker material failure when the initial crack is larger. This is similar to the study by Amsterdam et al., [56] who found larger crack length weaken the material toughness more.

4.4 Propagation Time and Strength Reduction on Structure Plate

The time required for cracks to propagate through ship structural materials is analyzed to assess long-term performance and durability. The analysis calculates crack propagation time based on cycles needed for crack extension, as shown in Figure 22. The longest propagation time, 9.32 years, occurred in the SA-C4 var-

iation, while the shortest, 1.44 years, occurred in the SA-C1 variation. Results show that thicker outer plates and cores slow crack propagation, while longer initial cracks accelerate it. For example, increasing core thickness from 15 mm to 24 mm increased propagation time, and the propagation time decreased with larger initial cracks, from 3.49 years (25 mm crack) to 1.44 years (75 mm crack). The shorter timespan for larger crack also found in study by Leheta et al. [41].

The structural strength analysis evaluates the effects of outer plate thickness, core thickness, and initial crack size on the stress within the core material of the ship plate. Results show that thinner outer plates tend to concentrate stress more heavily in the core, particularly when larger initial cracks are present. This suggests that thinner outer plates may weaken structural integrity, accelerating crack propagation and reducing overall strength. In contrast, configurations with thicker outer and core plates distribute stress more evenly, improving structural toughness and reducing the risk of failure. The Stress Reduction Factor (SRF) is used to compare the stress in the damaged structure to the stress under normal conditions, with the maximum SRF value set at 34%.

Thinner configurations, such as SA-C1 (4 mm outer plate) and SB-C1 (6 mm outer plate), show higher SRF values, indicating a greater reduction in strength as the initial crack size increases. For instance, SA-C1 and SB-C1 exhibit SRF values ranging from 39% to 51%, exceeding the maximum allowable limit. On the other hand, configurations with thicker face and bottom plates, like SA-C4

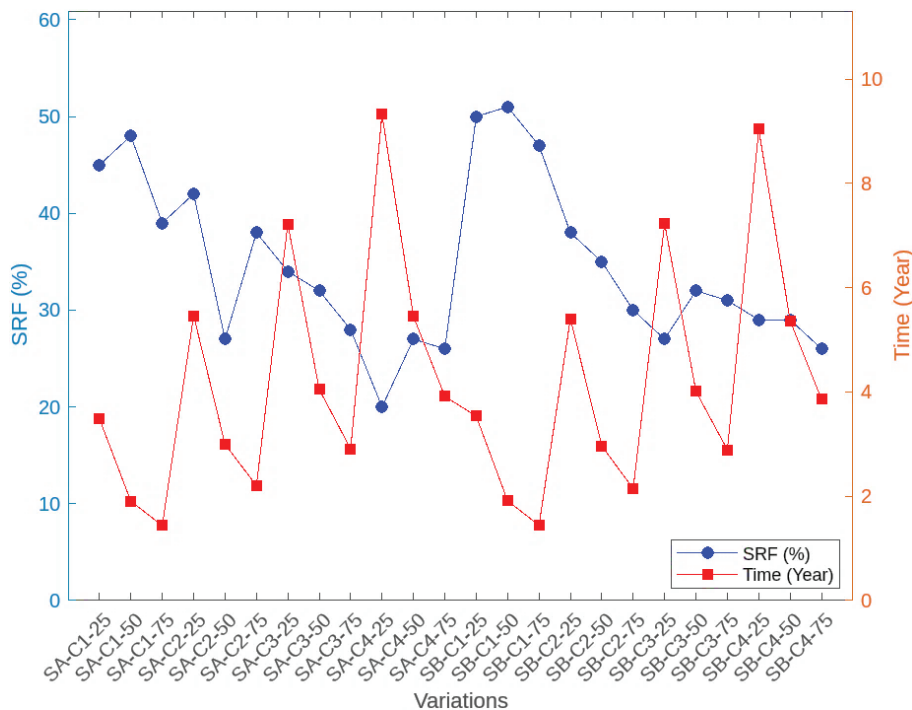


Figure 22 The strength reduction factor and propagation time for structure variations

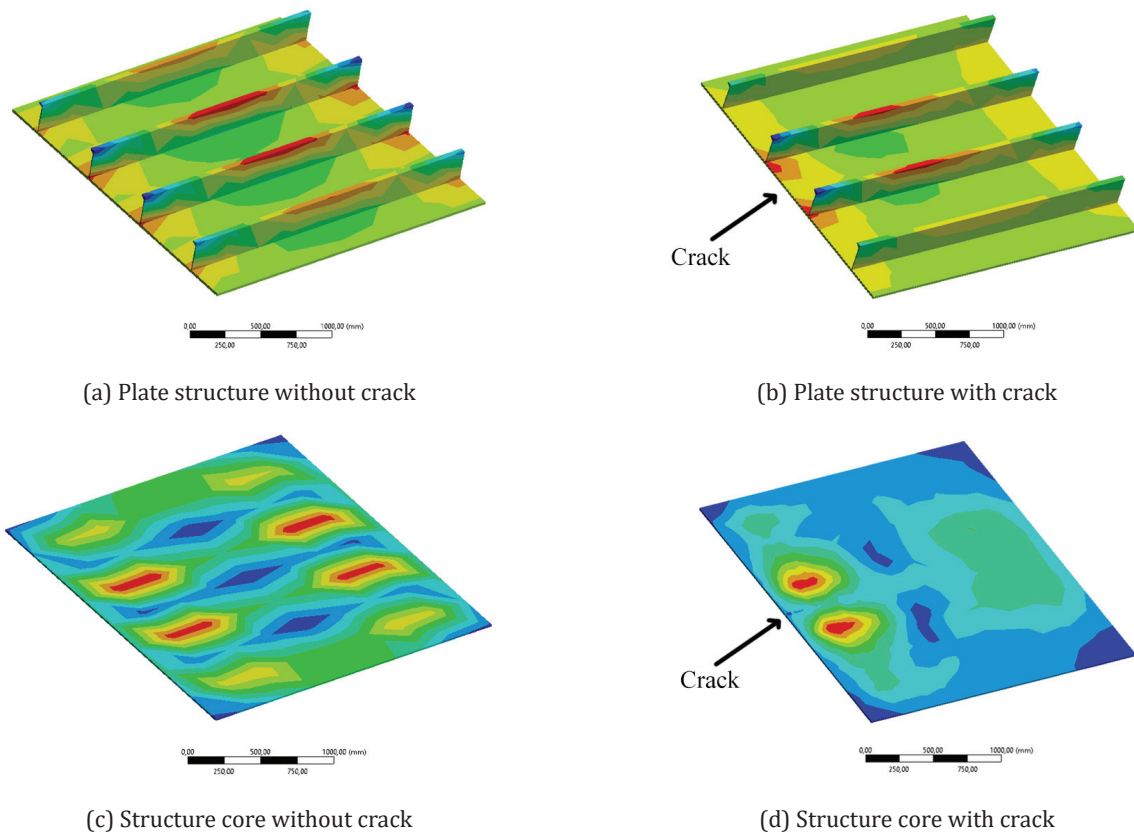


Figure 23 The comparison of plate loading under normal conditions and with the addition of crack

and SB-C4 (24 mm outer plate), maintain SRF values within or below the acceptable limit across different crack sizes, demonstrating enhanced structural strength and crack resistance.

Core thickness also plays a vital role in determining strength. The comparison of normal plate loading with damaged plate loading, shown in Figure 23, reveals how damage alters material response. The finite element analysis visualizes stress concentration using color contours, where lower stress is represented by dark colors and higher stress by lighter ones (yellow to red). The critical stress is concentrated around the crack tips, highlighting these areas as structural weak points. This pattern is also visible in the core, where stress around the crack is significantly higher than in undamaged areas, underlining the impact of cracks on both the plate and core structure. Significant area of stress around damaged point can be found in Tuswan et al., [57] study as well.

5 Conclusions

The research on the side plates of a ship experiencing damage aimed to analyze the material's damage characteristics, emphasizing the urgency of assessing crack propagation in sandwich panel structures to pre-

vent structural failure. Given the vulnerability of low-density steel-polyurethane elastomer sandwich panels, understanding the mechanisms of crack growth is essential for ensuring structural reliability in ship applications. Numerical simulation, supported with experimental data, was employed to simulate crack propagation behavior under operational loads. The results revealed that cracks tend to move inward toward the structure, aligned with the wave load direction. Variations in face/bottom plate thickness, core thickness, and initial crack length significantly influenced both crack propagation rate and total crack extension. Specifically, increasing the core thickness from 15 mm to 24 mm reduced the crack propagation rate by up to 28% and increased crack extension resistance by up to 54%, with an average improvement of around 30%. Thicker face and bottom plates also contributed to a noticeable reduction in propagation rate. Meanwhile, reducing the initial crack length from 75 mm to 25 mm decreased the propagation rate by approximately 73%, demonstrating the critical impact of early crack size on structural performance. Additionally, damage to the sandwich structure caused notable stress redistribution around the crack zone, influencing the structural response under load. The study also found that increasing core and face-plate thickness, along with reducing initial crack size,

consistently led to lower strength reduction factor (SRF) values and extended crack growth times. The study successfully met its objectives by identifying the dominant factors influencing crack propagation and quantifying their impact under operational conditions. Numerical predictions were supported by experimental validation, reinforcing the accuracy of the model. These findings provide a practical basis for optimizing sandwich panel configurations in shipbuilding to enhance structural performance and service life.

Funding: The research presented in the manuscript did not receive any external funding.

Acknowledgements: The first author expresses sincere appreciation to the ITS Naval Architecture Department for the tuition support received during the Master's program, which significantly contributed to the development of this research paper.

Author Contributions: Husein Syahab: Conceptualization, Data curation, Formal analysis, Investigation, Methodology, Validation, Visualization, Writing – original draft; Achmad Zubaydi: Conceptualization, Investigation, Methodology, Validation, Supervision, Writing – review & editing; Heni Siswanti: Conceptualization, Data curation, Formal analysis, Investigation, Methodology, Resources, Validation; Rizky Chandra Ariesta: Conceptualization, Methodology, Resources, Validation, Supervision, Writing – review & editing.

References

- [1] Ismail, A., Zubaydi, A., Piscesa, B., Tuswan, T. (2023) A novel fiberglass-reinforced polyurethane elastomer as the core sandwich material of the ship-plate system. *J Mech Behav Mater.* 32. <https://doi.org/10.1515/jmbm-2022-0288>
- [2] Knott, J.F. (1973) *Fundamentals of Fracture Mechanics*. Butterworths, London
- [3] Xu, G., Qin, K., Yan, R., Dong, Q. (2022) Research on failure modes and ultimate strength behavior of typical sandwich composite joints for ship structures. *International Journal of Naval Architecture and Ocean Engineering.* 14, 100428. <https://doi.org/10.1016/j.IJNAOE.2021.100428>
- [4] Li, M., Yan, R., Shen, W., Qin, K., Li, J., Liu, K. (2022) Fatigue characteristics of sandwich composite joints in ships. *Ocean Engineering.* 254. <https://doi.org/10.1016/j.oceaneng.2022.111254>
- [5] Zenkert, D. (2009) Damage Tolerance of Naval Sandwich Panels. In: *Major Accomplishments in Composite Materials and Sandwich Structures*. pp. 279–303. Springer Netherlands, Dordrecht
- [6] Ariesta, R.C., Zubaydi, A., Ismail, A., Tuswan, T. (2021) Damage evaluation of sandwich material on side plate hull using experimental modal analysis. *Mater Today Proc.* 47, 2310–2314. <https://doi.org/10.1016/J.MAT-PR.2021.04.293>
- [7] Ismail, A., Zubaydi, A., Piscesa, B., Ariesta, R.C., Tuswan (2020) Vibration-based damage identification for ship sandwich plate using finite element method. *Open Engineering.* 10, 744–752. <https://doi.org/10.1515/eng-2020-0086>
- [8] Ismail, A., Zubaydi, A., Piscesa, B., Panangian, E., Ariesta, R.C., Tuswan, T. (2021) A comparative study of conventional and sandwich plate side-shell using finite element method. *IOP Conf Ser Mater Sci Eng.* 1034, 012027. <https://doi.org/10.1088/1757-899X/1034/1/012027>
- [9] Ariesta, R.C., Zubaydi, A., Ismail, A., Tuswan, Al-Syachri, M.Z. (2021) Identification of damage in a ship hull sandwich plate by natural frequency. *IOP Conf Ser Mater Sci Eng.* 1034, 012012. <https://doi.org/10.1088/1757-899X/1034/1/012012>
- [10] Odessa, I., Frostig, Y., Rabinovitch, O. (2020) Dynamic interfacial debonding in sandwich panels. *Compos B Eng.* 185, 107733. <https://doi.org/10.1016/j.compositesb.2019.107733>
- [11] Wang, M., Li, Y., Luo, H., Zheng, X., Li, Z. (2022) Experiment and Numerical Simulation of Damage Progression in Transparent Sandwich Structure under Impact Load. *Materials.* 15, 3809. <https://doi.org/10.3390/ma15113809>
- [12] Li, P., Liu, S., Lu, Z. (2017) Experimental Study on the Performance of Polyurethane-Steel Sandwich Structure under Debris Flow. *Applied Sciences.* 7, 1018. <https://doi.org/10.3390/app7101018>
- [13] Chernysh, A.A., Yakovlev, S.N. (2019) An Experimental Study of the Deformation of Polyurethane Elastomers Applied in the Ship's Shock-Absorbers. *Vestnik Gosudarstvennogo universiteta morskogo i rechnogo flota imeni admirala S. O. Makarova.* 11, 534–542. <https://doi.org/10.21821/2309-5180-2019-11-3-534-542>
- [14] Ismail, A., Zubaydi, A., Piscesa, B., Tuswan, T., Chandra, A. (2021) Study of sandwich panel application on side hull of crude oil tanker. *Journal of Applied Engineering Science.* 19, 1090–1098. <https://doi.org/10.5937/jaes0-30373>
- [15] Sharma, S.C., Krishna, M., Murthy, H.N.N., Sathyamoorthy, M., Bhattacharya, D. (2004) Fatigue Studies of Polyurethane Sandwich Structures. *J Mater Eng Perform.* 13, 637–641. <https://doi.org/10.1361/10599490420052>
- [16] Khan, A.M., Liang, L., Mia, M., Gupta, M.K., Wei, Z., Jamil, M., Ning, H. (2021) Development of process performance simulator (PPS) and parametric optimization for sustainable machining considering carbon emission, cost and energy aspects. *Renewable and Sustainable Energy Reviews.* 139, 110738. <https://doi.org/https://doi.org/10.1016/j.rser.2021.110738>
- [17] Ariesta, R.C., Zubaydi, A., Ismail, A., Tuswan, T. (2022) Identification of Damage Size Effect of Natural Frequency on Sandwich Material using Free Vibration Analysis. *Naše more.* 69, 1–8. <https://doi.org/10.17818/NM/2022/1.1>
- [18] Dhaliwal, G.S., Newaz, G.M. (2020) Flexural Response of Degraded Polyurethane Foam Core Sandwich Beam with Initial Crack between Facesheet and Core. *Materials.* 13, 5399. <https://doi.org/10.3390/ma13235399>
- [19] Shen, W., Luo, B., Yan, R., Zeng, H., Xu, L. (2017) The mechanical behavior of sandwich composite joints for ship structures. *Ocean Engineering.* 144, 78–89. <https://doi.org/10.1016/j.oceaneng.2017.08.039>

- [20] Babae Kashani, H., Shariati, M., Tahani, M., Zamani, P. (2025) Experimental and numerical investigation on failure of PVC foam core tapered sandwich composites under four-point bending. *Eng Fail Anal.* 173, 109450. <https://doi.org/10.1016/j.engfailanal.2025.109450>
- [21] Thiruvannamalai, M., Venkatesan, P.V., Chellapandian, M. (2024) Fatigue Life Predictions Using a Novel Adaptive Meshing Technique in Non-Linear Finite Element Analysis. *Buildings.* 14, 3063. <https://doi.org/10.3390/buildings14103063>
- [22] Savari, A. (2025) Crack assessment in spiral-welded pipelines repaired by composite patch: A SMART and failure assessment diagram approach. *Journal of Pipeline Science and Engineering.* 5, 100222. <https://doi.org/10.1016/j.jpse.2024.100222>
- [23] Alshoabi, A.M., Fageehi, Y.A. (2020) Numerical Analysis of Fatigue Crack Growth Path and Life Predictions for Linear Elastic Material. *Materials.* 13, 3380. <https://doi.org/10.3390/ma13153380>
- [24] Lameiras, R., Barros, J., Azenha, M., Valente, I.B. (2013) Development of sandwich panels combining fibre reinforced concrete layers and fibre reinforced polymer connectors. Part II: Evaluation of mechanical behaviour. *Compos Struct.* 105, 460–470. <https://doi.org/10.1016/j.compstruct.2013.06.015>
- [25] Nozaki, M., Sakane, M., Fujiwara, M. (2020) Low cycle fatigue testing using miniature specimens. *Int J Fatigue.* 137, 105636. <https://doi.org/10.1016/j.ijfatigue.2020.105636>
- [26] Wu, W.F., Ni, C.C. (2004) Probabilistic models of fatigue crack propagation and their experimental verification. *Probabilistic Engineering Mechanics.* 19, 247–257. <https://doi.org/10.1016/j.probengmech.2004.02.008>
- [27] Zubaydi, A., Budipriyanto, A. (2020) *Sandwich Material: Theory, Design, and Application.* Airlangga University Press, Surabaya
- [28] Siswanti, H., Muhammad Musta'in, Trisriandinda P, Arisessy Mulananda (2022) Study of the Use of Steel-Based Hybrid Sandwich Plate ASTM A36 with Polyurethane Elastomer Core Material in Ship Construction. *Jurnal Inovtek Polbeng.* 12.
- [29] Tsui, T.Y., Griffin, A.J., Fields, R., Jacques, J.M., McKerrow, A.J., Vlassak, J.J. (2006) The effect of elastic modulus on channel crack propagation in organosilicate glass films. *Thin Solid Films.* 515, 2257–2261. <https://doi.org/10.1016/j.tsf.2006.06.022>
- [30] Greaves, G.N., Greer, A.L., Lakes, R.S., Rouxel, T. (2011) Poisson's ratio and modern materials. *Nat Mater.* 10, 823–837. <https://doi.org/10.1038/nmat3134>
- [31] Rinker, M., Zahlen, P.C., John, M., Schäuble, R. (2012) Investigation of sandwich crack stop elements under fatigue loading. *Journal of Sandwich Structures & Materials.* 14, 55–73. <https://doi.org/10.1177/1099636211406425>
- [32] Sharma, S.C., Murthy, H.N.N., Krishna, M. (2004) Interfacial Studies in Fatigue Behavior of Polyurethane Sandwich Structures. *Journal of Reinforced Plastics and Composites.* 23, 893–903. <https://doi.org/10.1177/0731684404033958>
- [33] Mohammadi, M.S., Nairn, J.A. (2017) Balsa sandwich composite fracture study: Comparison of laminated to solid balsa core materials and debonding from thick balsa core materials. *Compos B Eng.* 122, 165–172. <https://doi.org/10.1016/j.compositesb.2017.04.018>
- [34] Mandal, N.R. (2017) *Ship Construction & Welding.* Springer, New Orleans
- [35] BKI (2023) *Rules of Hull.* Biro Klasifikasi Indonesia, Indonesia
- [36] Bulatović, S., Aleksić, V., Milović, L., Zečević, B. (2022) Application of Paris' law under variable loading. *FME Transactions.* 50, 72–78. <https://doi.org/10.5937/fme2201072B>
- [37] Ye, H., Huang, R., Zhou, Y., Liu, J. (2022) Calibration of Paris law constants for crack propagation analysis of damaged steel plates strengthened with prestressed CFRP. *Theoretical and Applied Fracture Mechanics.* 117, 103208. <https://doi.org/10.1016/j.tafmec.2021.103208>
- [38] Syahab, H., Zubaydi, A., Ariesta, R.C., Misbah, M.N., Sujiantanti, S.H., Putranto, T., Setyawan, D., Azary, F.Q. (2023) Fatigue Crack Growth on Ship Polyurethane-Steel Sandwich Plate. In: *International Conference on Ship and Offshore Technology (Accepted Publication).* Royal Institute of Naval Architects, Jakarta
- [39] Zhang, J., Zhao, J.X. (2008) Strength reduction factor (R factor) model and inelastic response spectra for forward-directivity ground motion.
- [40] Li, T., Lie, S. (2019) Strength Reduction Factors for Cracked Multi-planar Tubular DT-joints. *KSCE Journal of Civil Engineering.* 23, 307–320. <https://doi.org/10.1007/s12205-018-0547-z>
- [41] Leheta, H.W., Elhewy, A.M.H., Younes, H.A. (2016) Analysis of Fatigue Crack Growth in Ship Structural Details. *Polish Maritime Research.* 23, 71–82. <https://doi.org/10.1515/pomr-2016-0023>
- [42] Logan, D.L. (2015) *A First Course in the Finite Element Method.* Cengage Learning, Boston
- [43] ANSYS (2020) *SMART Fracture.*
- [44] Alshoabi, A.M. (2022) Fatigue Crack Growth Analysis under Constant Amplitude Loading Using Finite Element Method. *Materials.* 15, 2937. <https://doi.org/10.3390/ma15082937>
- [45] Fageehi, Y.A., Alshoabi, A.M. (2024) Investigating the Influence of Holes as Crack Arrestors in Simulating Crack Growth Behavior Using Finite Element Method. *Applied Sciences.* 14, 897. <https://doi.org/10.3390/app14020897>
- [46] Zhu, F., Liu, H., Yao, L., Mei, G. (2021) Study on the maximum tangential strain criterion for the initiation of the wing-crack under uniaxial compression. *Theoretical and Applied Fracture Mechanics.* 116, 103085. <https://doi.org/10.1016/j.tafmec.2021.103085>
- [47] Hughes, O.F., Paik, J.K. (2010) *Ship Structural Analysis and Design.* Society of Naval Architects and Marine Engineers, New Jersey
- [48] Siswanti, H., Zubaydi, A., Pisceca, B., Syahab, H., Ariesta, R.C. (2025) Study of polyurethane elastomer cores interfacial fracture resistance of the sandwich materials for ship structures. *IOP Conf Ser Earth Environ Sci.* 1461, 012005. <https://doi.org/10.1088/1755-1315/1461/1/012005>
- [49] Jameel, A., Harmain, G.A. (2020) Effect of material irregularities on fatigue crack growth by enriched techniques. *International Journal for Computational Methods in Engineering Science and Mechanics.* 21, 109–133. <https://doi.org/10.1080/15502287.2020.1772902>

- [50] Pyrzowski, Ł., Sobczyk, B. (2020) Local and global response of sandwich beams made of GFRP facings and PET foam core in three point bending test. *Compos Struct.* 241, 112122. <https://doi.org/10.1016/j.compstruct.2020.112122>
- [51] Sanjaya, Y., Prabowo, A.R., Imaduddin, F., Binti Nordin, N.A. (2021) Design and Analysis of Mesh Size Subjected to Wheel Rim Convergence Using Finite Element Method. *Procedia Structural Integrity.* 33, 51–58. <https://doi.org/10.1016/j.prostr.2021.10.008>
- [52] Kim, Y.J., Yoshitake, I., Liu, R. (2014) Composite hull structures subjected to wave-induced slamming impact. *Journal of Reinforced Plastics and Composites.* 33, 3–13. <https://doi.org/10.1177/0731684413499831>
- [53] Zhao, W., Leira, B.J., Feng, G., Gao, C., Cui, T. (2021) A reliability approach to fatigue crack propagation analysis of ship structures in polar regions. *Marine Structures.* 80, 103075. <https://doi.org/10.1016/j.marstruc.2021.103075>
- [54] Soleymani, M., Tahani, M., Zamani, P. (2021) On the influence of resin pocket area on the failure of tapered sandwich composites. *Advances in Structural Engineering.* 24, 42–51. <https://doi.org/10.1177/1369433220940816>
- [55] Zhou, C., He, J. (2023) Mixed mode fracture toughness and mode mixity analysis of face/core debonds in a single-leg sandwich bending specimen. *Theoretical and Applied Fracture Mechanics.* 124, 103813. <https://doi.org/10.1016/j.tafmec.2023.103813>
- [56] Amsterdam, Emiel., Wiegman, J.W., Nawijn, Marco., De Hosson, J. Th.M. (2022) The effect of crack length and maximum stress on the fatigue crack growth rates of engineering alloys. *Int J Fatigue.* 161, 106919. <https://doi.org/10.1016/j.ijfatigue.2022.106919>
- [57] Tuswan, T., Zubaydi, A., Piscesa, B., Ismail, A., Ariesta, R.C., Prabowo, A.R. (2022) A numerical evaluation on nonlinear dynamic response of sandwich plates with partially rectangular skin/core debonding. *Curved and Layered Structures.* 9, 25–39. <https://doi.org/10.1515/cls-2022-0003>